*minerals*

MDPI

*Article*

# Dissolution and Passivation Mechanism of Chalcopyrite during Pressurized Water Leaching

**Lishuai Jiang [1], Hongguang Leng [2] and Baisui Han [1,*]**

[1] School of Mining Engineering, University of Science and Technology Liaoning, Anshan 114051, China; jiangtong62022@163.com
[2] Daye Nonferrous Metals Group Holdings Co., Ltd., Huangshi 435100, China; 320195500020@ustl.edu.cn
* Correspondence: baisui.han@ustl.edu.cn; Tel.: +86-0412-5929488

**Abstract:** In this study, chemical leaching, XRD, SEM, and XPS analyses were conducted to investigate the dissolution and passivation mechanisms of chalcopyrite under pressurized oxidative conditions in water. The chemical leaching results showed that the chalcopyrite could be dissolved by pressurized leaching without any acid addition, i.e., in an $O_2$–$H_2O$ system, and the copper leaching rate reached 96.4% under the optimal conditions of 180 °C, 1.5 MPa, 900 rpm, and 90 min. The XRD, SEM, and XPS data suggested that a large proportion of the chalcopyrite dissolved in solution via the mineral phase transformation of $CuFeS_2 \rightarrow Cu^{2+}$ and $CuFeS_2 \rightarrow CuS \rightarrow Cu^{2+}$, i.e., some of the chalcopyrite directly leached into solution as $Cu^{2+}$, and some of it was first converted to CuS and then to $Cu^{2+}$. The primary passivation layers during the chalcopyrite pressurized water leaching were hematite, pyrite, and covellite; however, none of them covered the un-leached mineral surface or inhibited chalcopyrite dissolution, as long as the agitation speed and leaching time were maintained over 700 rpm and 60 min, respectively. Finally, a model of chalcopyrite's dissolution and passivation mechanism during pressurized water leaching was proposed.

**Keywords:** chalcopyrite; water; pressurized leaching; mechanisms; passivation

check for updates

**Citation:** Jiang, L.; Leng, H.; Han, B. Dissolution and Passivation Mechanism of Chalcopyrite during Pressurized Water Leaching. *Minerals* **2023**, *13*, 996. https://doi.org/10.3390/min13080996

Academic Editor: Jean-Francois Blais

Received: 4 July 2023
Revised: 21 July 2023
Accepted: 26 July 2023
Published: 27 July 2023

**Copyright:** © 2023 by the authors. Licensee MDPI, Basel, Switzerland. This article is an open access article distributed under the terms and conditions of the Creative Commons Attribution (CC BY) license (https://creativecommons.org/licenses/by/4.0/).

## 1. Introduction

Chalcopyrite ($CuFeS_2$) is one of the significant copper-bearing minerals in nature and is the primary mineral used for the commercial production of copper via the pyrometallurgical process [1,2], such as smelting. Hydrometallurgical copper extraction is an alternative to the pyrometallurgical process, which is more attractive from many perspectives, such as the ability to deal with a large spectrum of impurities, applicability to low-grade minerals, and feasibility of low-capacity operation [3]. Various studies have considered the dissolution of chalcopyrite under different pressures, e.g., atmospheric [4–6] and high pressure [7–10], and in different media, e.g., sulfuric acid [9,11,12], chlorides [13,14], nitrates [15,16], and ammonia [17]. It must be noted that using those oxidants could improve the leaching efficiency of chalcopyrite; however, it faces economic problems due to the high acid consumption and environmental problems caused by the waste acid. Perhaps surprisingly, only little attention has been paid to pressurized water leaching [8,18]. Ji et al. have studied the behavior and kinetics of copper during the pressurized oxidative leaching of complex chalcopyrite without acid [19]. Further insight is sought with regards to passivation, phase transition, and leaching mechanism by using analytical techniques.

The present study investigates the possibility of efficient chalcopyrite leaching in a pressurized water system. Chemical leaching, X-ray diffraction, and X-ray photoelectron spectroscopy analyses were conducted to understand chalcopyrite's dissolution and passivation mechanisms under pressurized oxidative conditions in water.

## 2. Materials and Methods

### *2.1. Materials*

Chalcopyrite ($CuFeS_2$) ore was obtained from a mine in Yunnan, China. The chalcopyrite was first dry-crushed to below 10 mm, and then the crushed mineral was "hand-picked" to reject any pieces containing visible non-sulfide mineral impurities. Then, the minerals were dry-screened to extract size fractions of −47 μm. The mineralogical and chemical studies on the ore sample were carried out by X-ray diffraction (XRD, D8 ADVANCE, Bruker, Germany) and X-ray fluorescence spectrometry (XRF, Bruker S8 TIGER, Bruker, Germany), respectively. The XRD pattern (see Figure 1) and the chemical analysis (see Table 1) confirmed that the chalcopyrite samples had excellent purity.

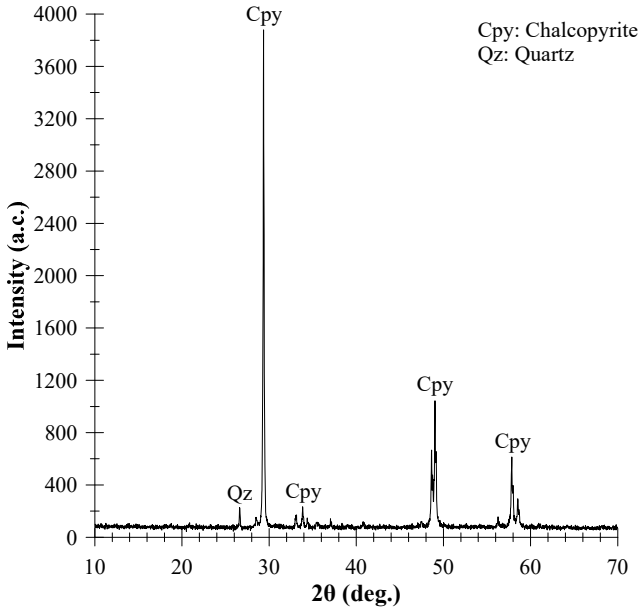



**Figure 1.** XRD patterns of the chalcopyrite sample.

**Table 1.** Chemical composition of chalcopyrite.

| Elements | Concentration (%) |
|---|---|
| S | 33.4 |
| Cu | 29.8 |
| Fe | 29.3 |

### *2.2. Methods*

All pressurized oxidative leaching experiments were conducted using a stainless-steel autoclave (Shanghai LABE Instrument Co., Ltd., Shanghai, China, AB-500) with a Teflon vessel (500 mL). First, 4 g of chalcopyrite sample were mixed with 150 mL of water in the Teflon vessel. The vessel containing a slurry sample was then put into the autoclave, followed by agitation using a magnetic impeller at speeds ranging from 300 to 900 rpm. The charged slurry/feed in the autoclave was heated to the required temperature (120–180 °C), and pure oxygen gas was injected into the vessel to maintain the target total pressure (sum of vapor and oxygen partial pressures: 0.8–2.0 MPa), and then the reaction proceeded further for a period ranging from 0 to 90 min. After the completion of pressurized oxidative leaching, the feed in the vessel was cooled down by a circulation water system and filtered through a 0.45 μm membrane to obtain pregnant leach solution (PLS) and solid residue, which were subjected to chemical and mineralogical analyses using ICP-OES (Jena Analytical Instruments Co., Ltd., PQ LC-Plasma Quant MS, Jena, Germany), XRD, X-ray photoelectron spectroscopy (XPS, Thermo Fisher Instrument Manufacturing Co., Ltd.,

ESCALAB 250Xi, Waltham, American), and scanning electron microscopy (SEM, ZEISS Co., Ltd., Sigma 500, Bruker, Germany), respectively. The following formula (Equation (1)) calculated the leaching rate of each metal ($R_m$) in the PLS after leaching:

$$R_m(\%) = \frac{C_L \cdot V_L}{C_F \cdot M_F} \times 100, \quad (1)$$

where $R_m$ is the metal leaching rate, %, $C_L$ and $C_F$ are the concentrations of metal in the PLS (mg/L) and feed (mg/kg), respectively. $V_L$ is the volume of the PLS (L), and $M_F$ is the dry mass of the feed (kg).

## 3. Results and Discussion

### *3.1. Pressurized Oxidative Water Leaching Study*

The pressurized oxidative leaching experiments using water were conducted at a variety of temperatures (120–180 °C), total pressures (1.0–2.0 MPa), agitation speeds (300–900 rpm), leaching times (30–90 min), and a fixed particle size of −47 μm. The results are given in Figure 2.

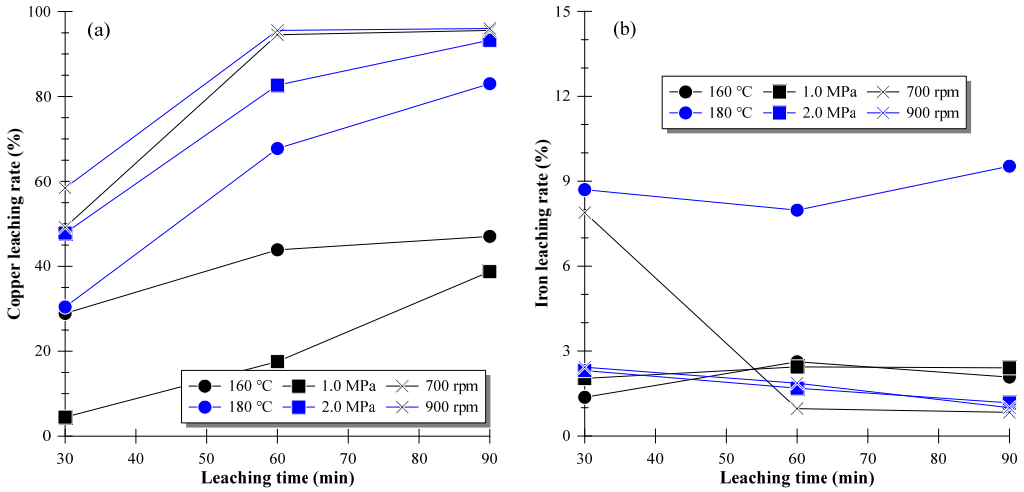



**Figure 2.** The (**a**) copper and (**b**) iron leaching rate in an $O_2$–$H_2O$ system under a variety of conditions: −47 μm, 160–180 °C, 1.0–2.0 MPa, and 700–900 rpm for 30–90 min.

It can be seen from the results in Figure 2 that the copper dissolution rate was relatively lower (<50%) when the temperature was set under 160 °C for 90 min of leaching. However, the leaching rate of copper reached about 83% when increasing the temperature to 180 °C within 90 min. In the case of the total pressure, the copper leaching rate was maintained at a relatively higher level once the setting was over 1.5 MPa, at which a leaching rate of 93.3% was obtained after 90 min of leaching. The agitation speed results showed that the stirring rate was an essential factor for the chalcopyrite leaching, and the dissolution rate of the copper was not significant at lower agitation speeds under 700 rpm. As a result, a maximum copper leaching rate of 96% was confirmed under the following optimal conditions: total pressure 2.0 MPa, temperature 180 °C, and agitation speed 900 rpm for 90 min. It must be pointed out that chalcopyrite is a refractory mineral in a hydro-environment due to the formation of a passivation layer (e.g., S); therefore, it is necessary to add some oxidants, such as sulfuric acid, hydrochloric acid, and nitric acid, to achieve efficient copper leaching. However, it was confirmed that chalcopyrite could be effectively extracted in an $O_2$–$H_2O$ system, i.e., without any addition of other oxidants. As seen in Figure 2, the temperature, total pressure, and agitation speed were the key factors of copper leaching from chalcopyrite, and the influence degree might be agitation speed > temperature > total pressure. Once the temperature, agitation speed, and total pressure were set to over 180 °C, 700 rpm, and 2.0 MPa, respectively, the copper was able to significantly dissolute from the

chalcopyrite into solution within 90 min. Interestingly, the iron leaching rate was always lower than 13% in all experimental sets; even that of copper maintained a very high level (over 90%). As reported by McDonald et al., there is an induction period during which iron is released before copper begins to appear in the solution at significant levels, i.e., the iron will be extracted from the structure of chalcopyrite earlier than copper [20]; however, the dissolved Fe ions will be rapidly hydrolyzed and present in the leaching residue. This is consistent with the Fe extraction results of this study and indicates that the dissolved Fe must be recomposed in a new form in the leaching residue.

### *3.2. XRD and SEM Study*

XRD was performed on a portion of the solid residues recovered from the leaching experiments that had the following conditions: particle size −47 μm, temperature 120–180 °C, total pressure 1.0–2.0 MPa, and agitation speed 300–900 rpm for 90 min of leaching. Figure 3a–l shows the diffraction patterns obtained.

The XRD patterns obtained under the conditions of 1.5 MPa, 500 rpm, and 120–180 °C are shown in Figure 3a–d. It can be seen that one hematite ($Fe_2O_3$) peak was observed at 120 °C; however, the primary phase was still chalcopyrite (Figure 3a), which is consistent with the leaching result, i.e., only 10% of the copper dissolved from the chalcopyrite. With the increasing leaching temperature, the primary phase of the solid changed to $Fe_2O_3$, and a peak of covellite (CuS) and pyrite ($FeS_2$) was detected at 160 °C (Figure 3c). In the case of 180 °C, only $Fe_2O_3$, CuS, and un-leached $CuFeS_2$ were found, and the $FeS_2$ confirmed at 160 °C disappeared (Figure 3d). When the conditions were fixed at 180 °C and 500 rpm with a variety of total pressures from 0.8–2.0 (see Figure 3e–h), once the pressure was set to 1.0 MPa, many CuS, $Fe_2O_3$, and $FeS_2$ peaks appeared in the solid residue (Figure 3f). However, both the CuS and $FeS_2$ peaks disappeared when increasing the total pressure to 2.0 MPa (Figure 3h), while the majority of the mineral phase was $Fe_2O_3$ and un-leached chalcopyrite. Figure 3i–l shows the XRD patterns of the residue observed at the fixed condition of 1.5 MPa and 180 °C while changing the agitation speed over a range of 300–900 rpm. As can be seen from Figure 3i, in addition to the original un-leached chalcopyrite, peaks of CuS and $Fe_2O_3$ were found, and the copper leaching rate was lower than 20%. However, the observed CuS peaks disappeared when increasing the agitation speed over 700 rpm, and the majority phase of the residue was changed to $Fe_2O_3$ (Figure 3k,l). All of the results suggested that chalcopyrite could be significantly dissolved without any addition of acid, using only water, while the essential conditions were set to over 1.5 MPa, 500 rpm, and 180 °C, respectively. However, it must be noted that all of the chalcopyrites might not be directly released from the surface and dissolved as $Cu^{2+}$. It is interesting to note that the pyrite and covellite peaks were confirmed in moderate experimental conditions, such as 160 °C (Figure 3e) and 1.0 MPa (Figure 3f), which was not part of the original mineral in the feed, i.e., a newly generated phase during chalcopyrite leaching.

The SEM–EDS study was conducted using the un-leached chalcopyrite sample and solid residues collected from the leaching under specific conditions, and the results are shown in Figures 4–7.

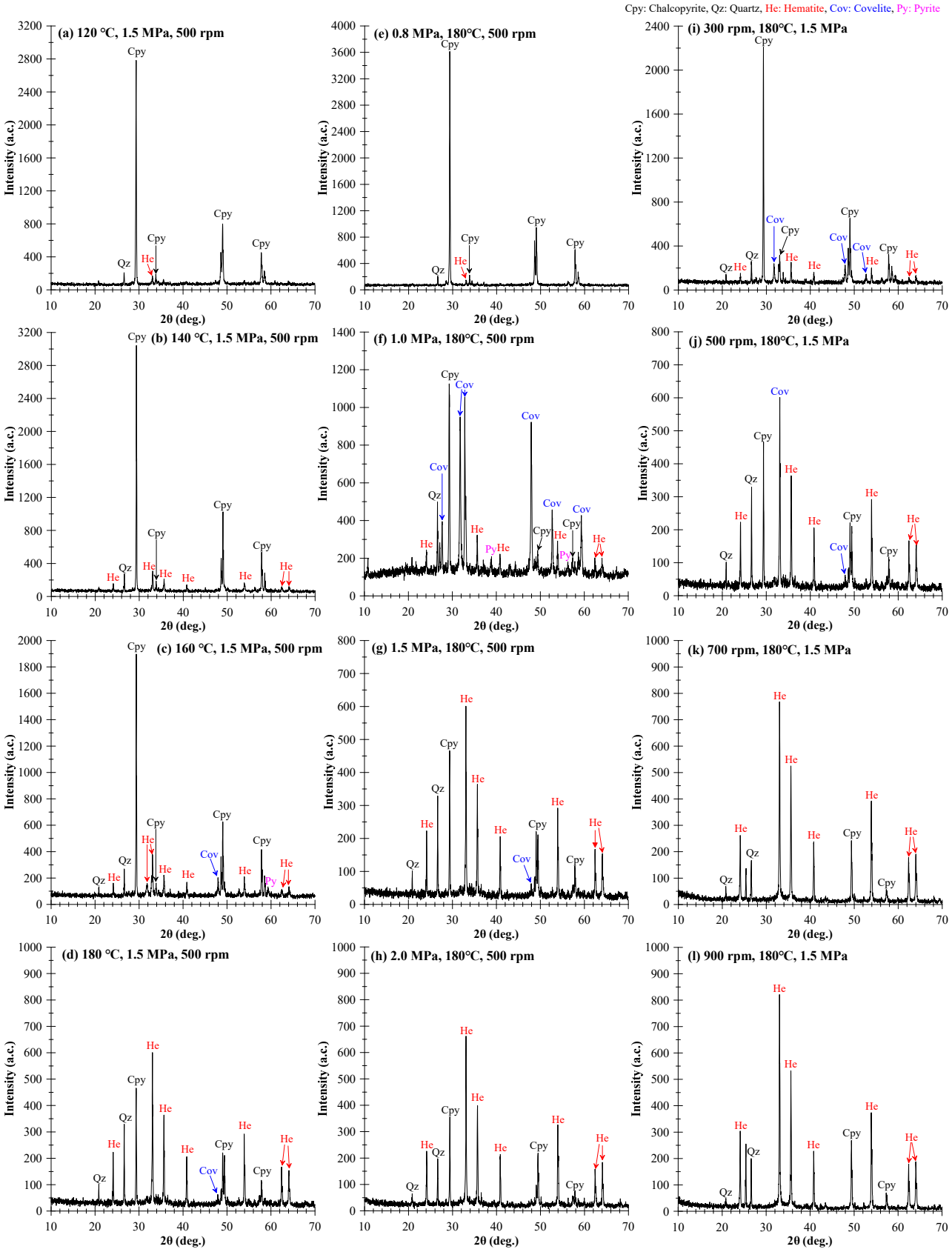



**Figure 3.** XRD patterns of leaching residue obtained at (**a**–**d**) 120, 140, 160, and 180 °C at 1.5 MPa and 500 rpm, (**e**–**f**) 0.8, 1.0, 1.5 and 2.0 MPa at 180 °C and 500 rpm, and (**i**–**l**) 300, 500, 700, and 900 rpm at 180 °C and 1.5 MPa, and −47 μm in water for 90 min.

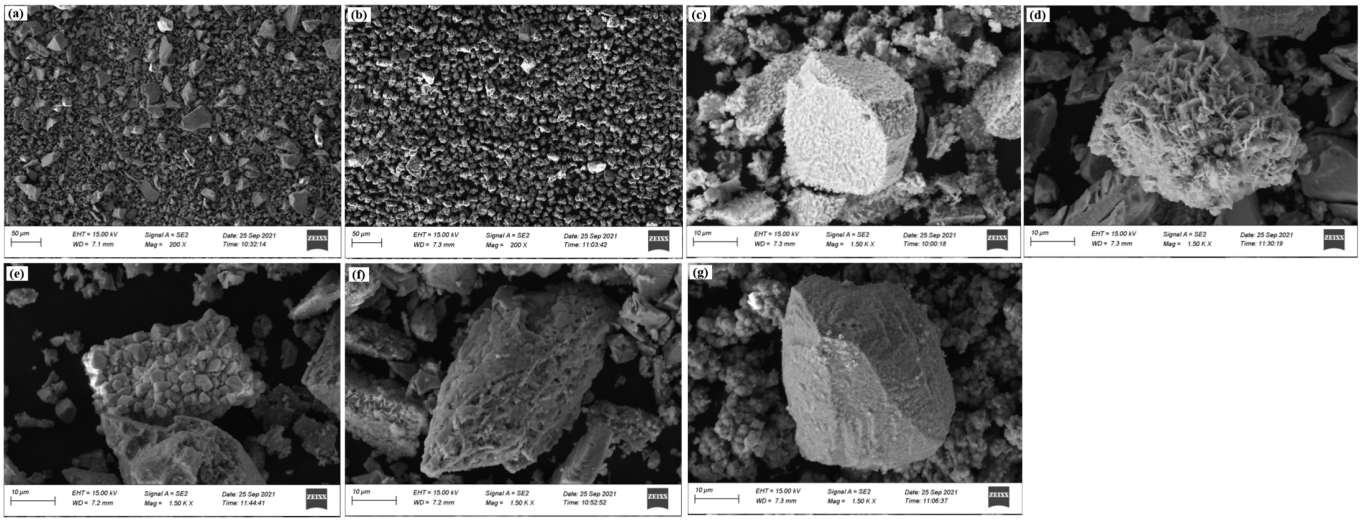



**Figure 4.** SEM observation of the (**a**) un-leached chalcopyrite, (**b**) residue obtained after leaching, and (**c**–**g**) enlarged points of the residue obtained from pressurized oxidative water leaching at 180 °C, −47 μm, 1.5 MPa, and 500 rpm for 90 min.

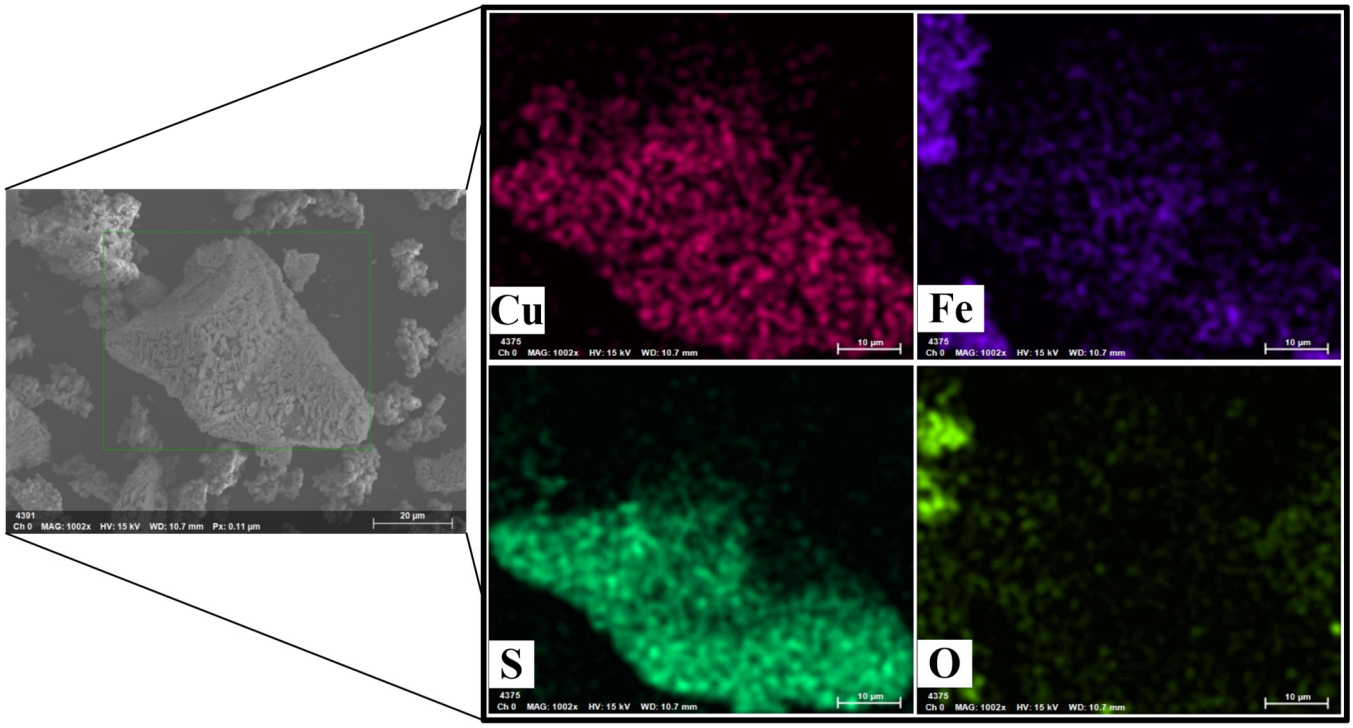



**Figure 5.** SEM–EDS observation of the residue obtained from pressurized oxidative water leaching at 180 °C, −47 μm, 1.5 MPa, and 500 rpm for 90 min.

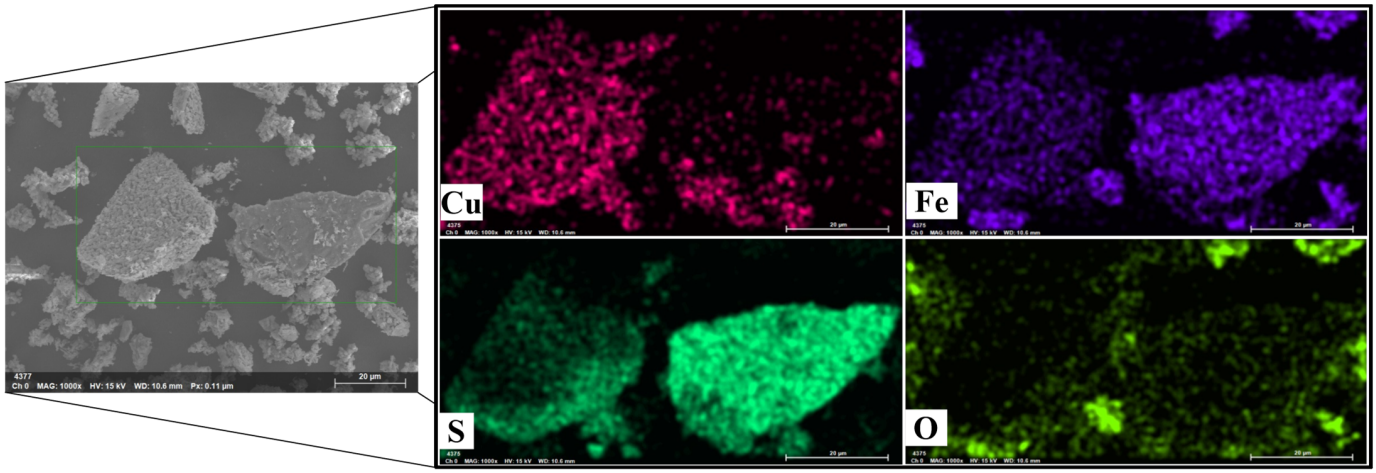



**Figure 6.** SEM observation of the residue obtained from pressurized oxidative water leaching at 180 °C, −47 μm, 1.5 MPa, and 500 rpm for 90 min.

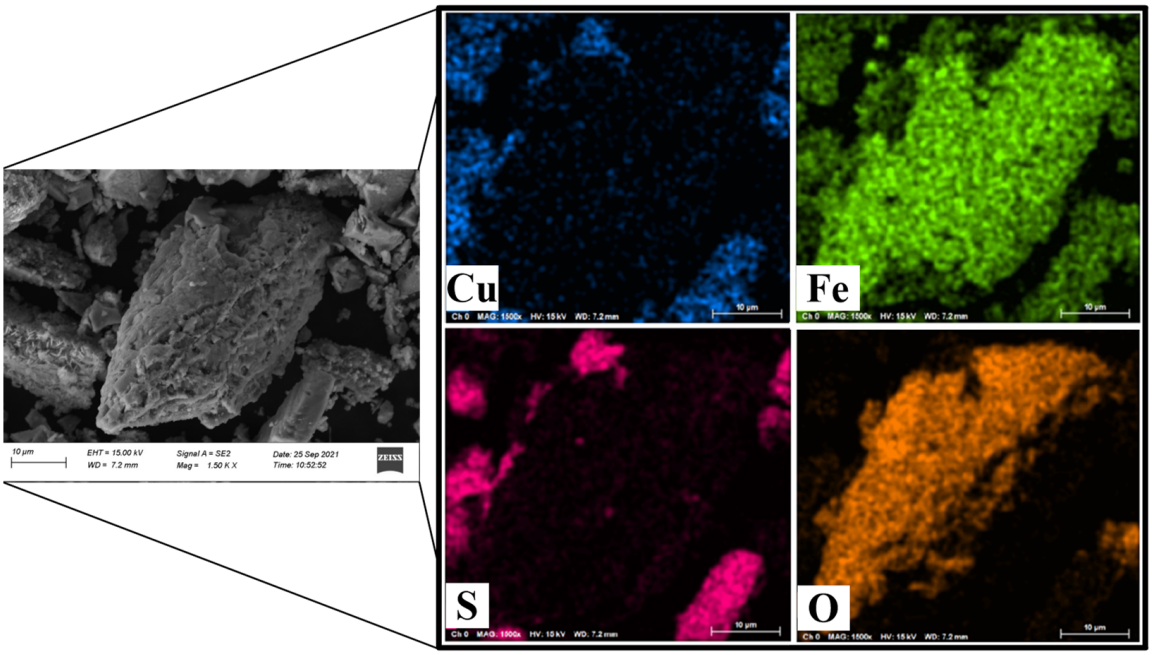



**Figure 7.** SEM observation of the residue obtained from pressurized oxidative water leaching at 180 °C, −47 μm, 1.5 MPa, and 700 rpm for 60 min.

It can be seen from Figure 4a that the particles of the original chalcopyrite sample are uneven, the surface of the mineral is relatively flat, and the particle size is finer than 50 μm, which is consistent with that of the feed sample (−47 μm). Obviously, the residue particle size became smaller and uniform (see Figure 4b) when the leaching conditions were 180 °C, 1.5 MPa, and 500 rpm in water for 90 min, indicating that most of the chalcopyrite was dissolved and some new mineral phase might have formed. It must be pointed out that some interesting particle types were detected, i.e., scaly structures (Figure 4c), flowerlike structures (Figure 4d), stacked structures (Figure 4e), honeycomb structures (Figure 4f), and multi-spherical structures (Figure 4g). From the EDS results given in Figures 5 and 6, the "scale" on the particle surface was mainly consistent with Cu and S elements, which refer to CuS or $CuS_2$. This phenomenon was also confirmed by the XRD analysis given in Figure 3. At the same time, an uncovered and un-leached Cu-Fe-S phase was found (Figures 5 and 6). The "multi-sphere" and "honeycomb" were confirmed as the Fe-O phase, which are located

at the top right of Figures 6 and 7, respectively, consisting of the results obtained from the XRD studies indicating that the primary Fe phase was hematite after leaching.

### *3.3. XPS Measurements*

XPS is a very useful surface analytical tool for mineral dissolution research to further explore the phase transformation and the composition of the passivation layer in the leaching process. In this section, the general XPS spectra of the original chalcopyrite sample and solid residues obtained after leaching at certain conditions were studied (particle size of −47 µm, temperature of 140–180 °C, the total pressure of 1.0–2.0 MPa, and agitation speed of 700 rpm for 30–90 min leaching), as well as the high-resolution spectra of copper (Cu), iron (Fe), and sulfur (S) species, and the results are given in Figures 8–13.

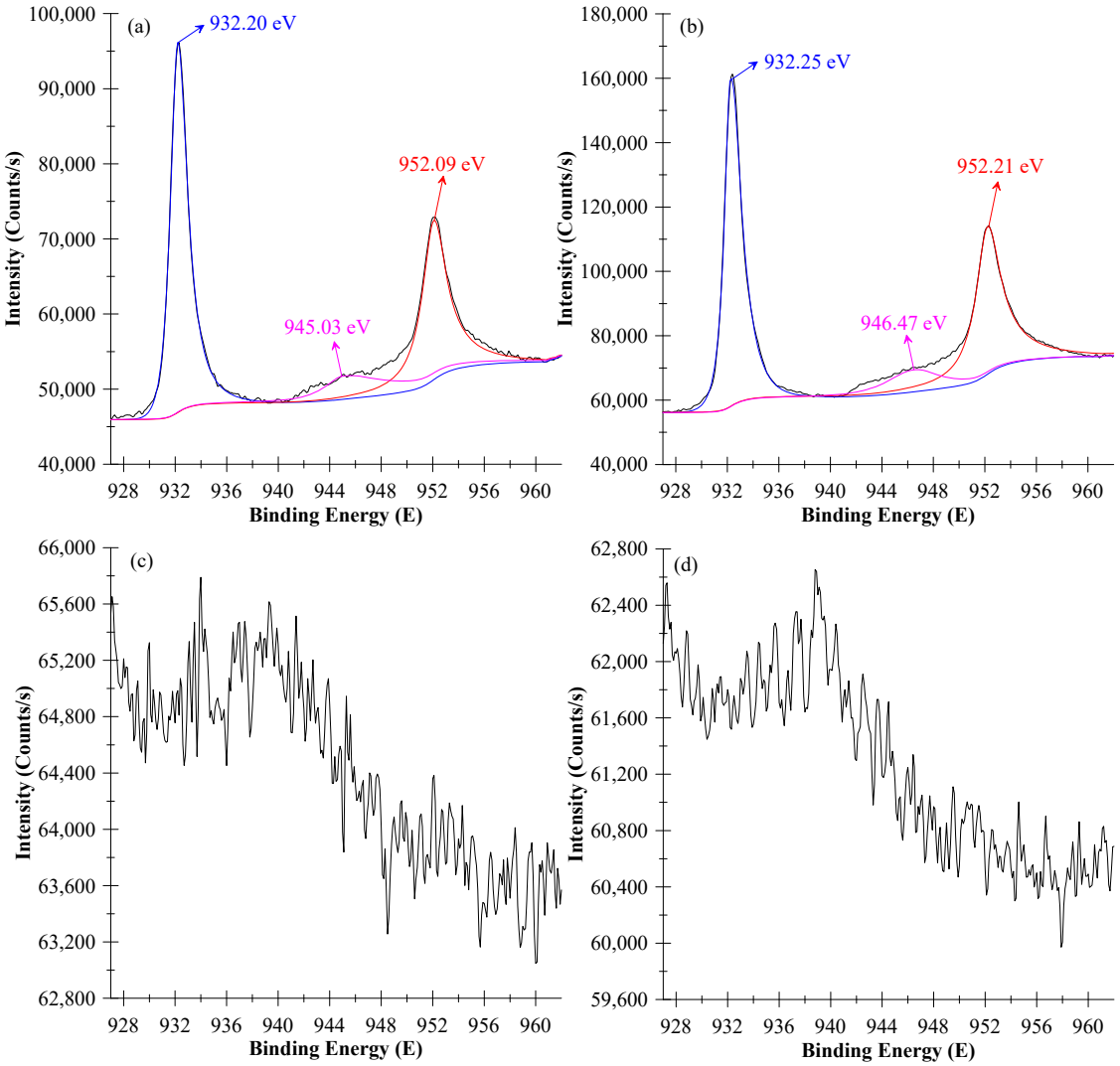



**Figure 8.** XPS spectrum of Cu 2p samples (**a**) before leaching, (**b**) after 30 min of leaching, (**c**) after 60 min of leaching, and (**d**) after 90 min of leaching at 180 °C, 1.5 MPa, and 700 rpm.

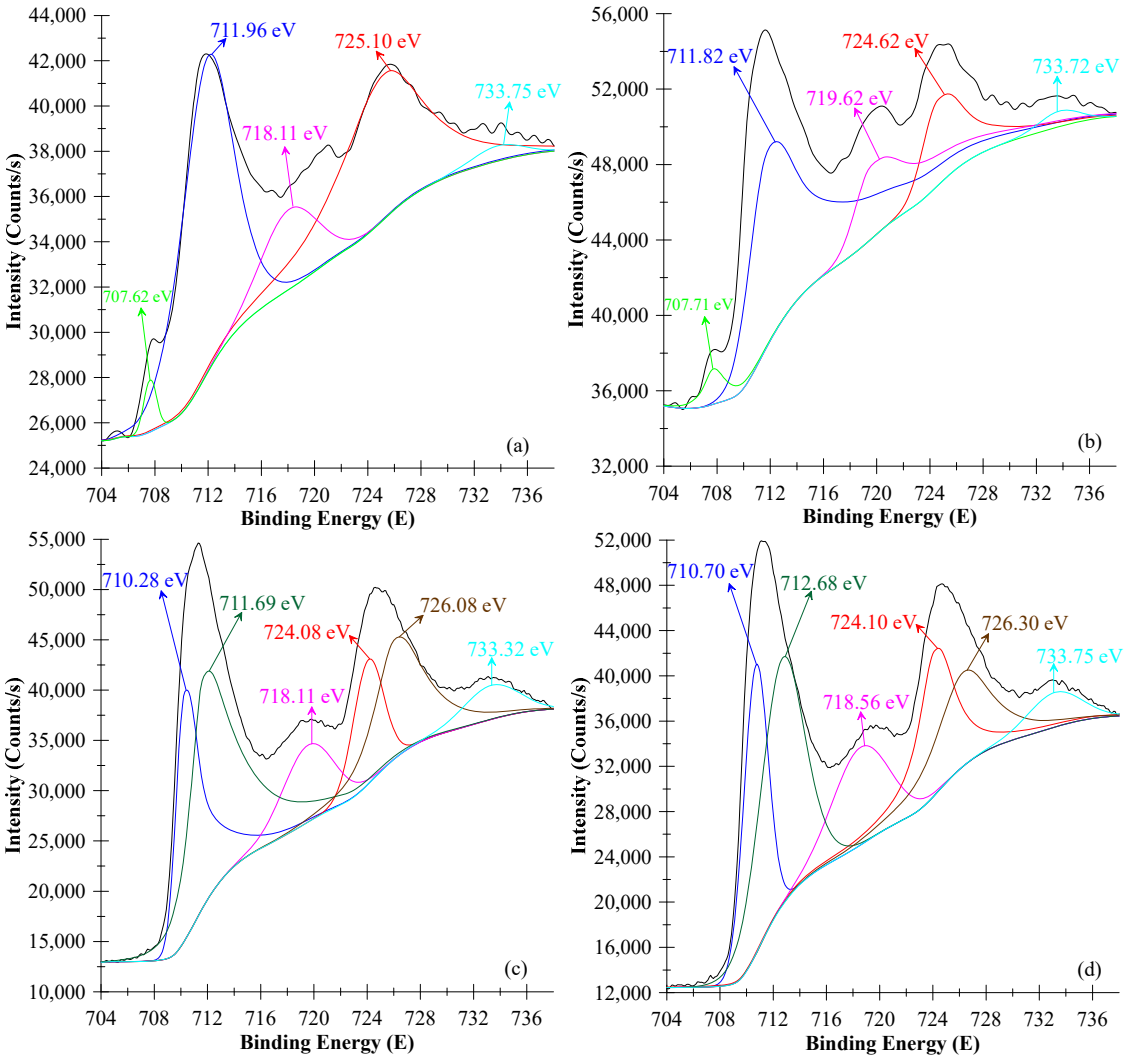



**Figure 9.** XPS spectrum of Fe 2p samples (**a**) before leaching, (**b**) after 30 min of leaching, (**c**) after 60 min of leaching, and (**d**) after 90 min of leaching at 180 °C, 1.5 MPa, and 700 rpm.

Chalcopyrite with a fresh surface, i.e., an un-leached sample, was analyzed by XPS, and the spectrum is provided in Figures 8a, 9a and 10a. It can be seen from Figure 8a that the binding energies of the peaks were in good agreement with the previous research [2,3,21,22], revealing that the Cu 2p 3/2 and Cu 2p 1/2 peaks were centered at 932.20 eV and 952.09 eV, respectively, which could be assigned to cuprous ($Cu^+$) species. As can be seen from Figure 8a, a satellite peak at 945.03 eV was found in the un-leached chalcopyrite surface, which might have resulted from the oxidation of the original sample. It has been reported that the Cu 2p3/2 peak, with the presence of a shake-up around 939.00–944.00 eV [22], is the major XPS characteristic of cupric ($Cu^{2+}$) species. Therefore, the presence of the $Cu^{2+}$-related peak at the binding energy of 945.03 eV suggested that both $Cu^+$ and $Cu^{2+}$ ions of copper were present in the chalcopyrite structure. This result is in agreement with the effective oxidation state of chalcopyrite being between $Cu^+Fe^{3+}(S^{2-})_2$ and $Cu^{2+}Fe^{2+}(S^{2-})_2$, which is caused by significant covalent bonding [6,23]. However, there are non-significant peaks found in the case of after 60 and 90 min leaching (Figure 8c,d) because most of the copper was dissolved into the pregnant leaching solution. Table 2 presents the copper auger spectrum (CuL3M45M45) excited with an X-ray, which was centered at 568.68 eV. This value was in excellent agreement with that measured by Ghahremaninezhad et al. and Wang et al., which was 568.65 eV, while the CuL3M45M45 values for the Cu-Cu bond, CuS, and $Cu_2S$ were 568.1, 568.5, and 569.5 eV, respectively [3,24].

**Table 2.** The binding energy of copper for un-leached chalcopyrite and solid residues.

| Leaching Conditions | Cu L3M45M45 |
|---|---|
| un-leached chalcopyrite | 568.63 |
| 180 °C, 1.5 MPa, 700 rpm, and −47 μm for 30 min | 568.55 |
| 180 °C, 1.5 MPa, 700 rpm, and −47 μm for 60 min | - |
| 180 °C, 1.5 MPa, 700 rpm, and −47 μm for 90 min | - |
| 140 °C, 1.5 MPa, 500 rpm, and −47 μm for 30 min | 568.87 |
| 160 °C, 1.5 MPa, 500 rpm, and −47 μm for 30 min | 568.72 |
| 180 °C, 1.5 MPa, 500 rpm, and −47 μm for 30 min | 568.83 |
| 180 °C, 0.8 MPa, 500 rpm, and −47 μm for 30 min | 568.47 |
| 180 °C, 1.0 MPa, 500 rpm, and −47 μm for 30 min | 568.70 |
| 180 °C, 2.0 MPa, 500 rpm, and −47 μm for 30 min | 568.72 |

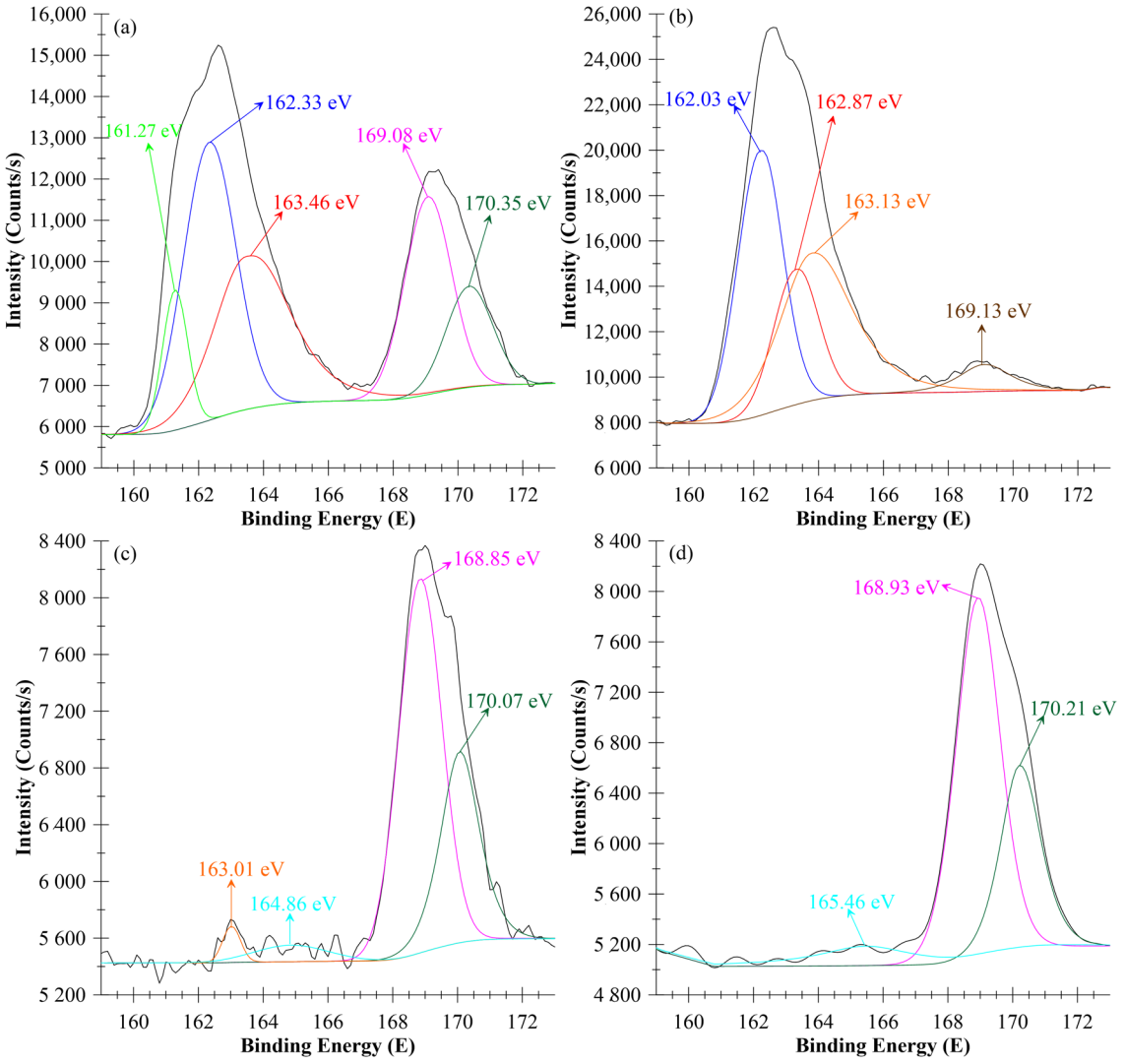



**Figure 10.** XPS spectrum of S 2p samples (**a**) before leaching, (**b**) after 30 min of leaching, (**c**) after 60 min of leaching, and (**d**) after 90 min of leaching at 180 °C, 1.5 MPa, and 700 rpm.

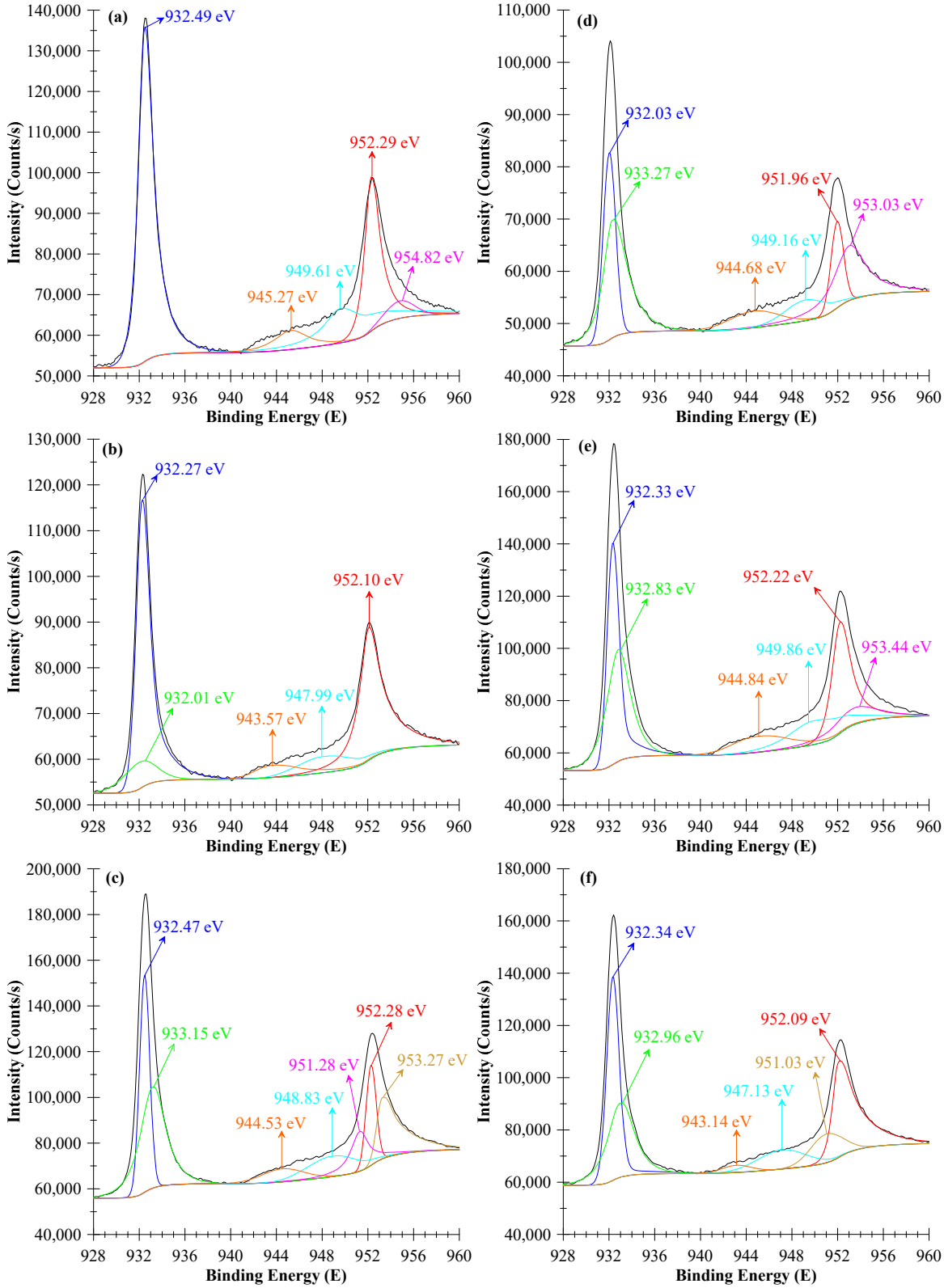



**Figure 11.** XPS spectrum of Cu 2p solid residues obtained at (**a**) 140 °C, (**b**) 160 °C, (**c**) 180 °C, (**d**) 0.8 MPa, (**e**) 1.0 MPa, and (**f**) 2.0 MPa at 700 rpm after 30 min of leaching.

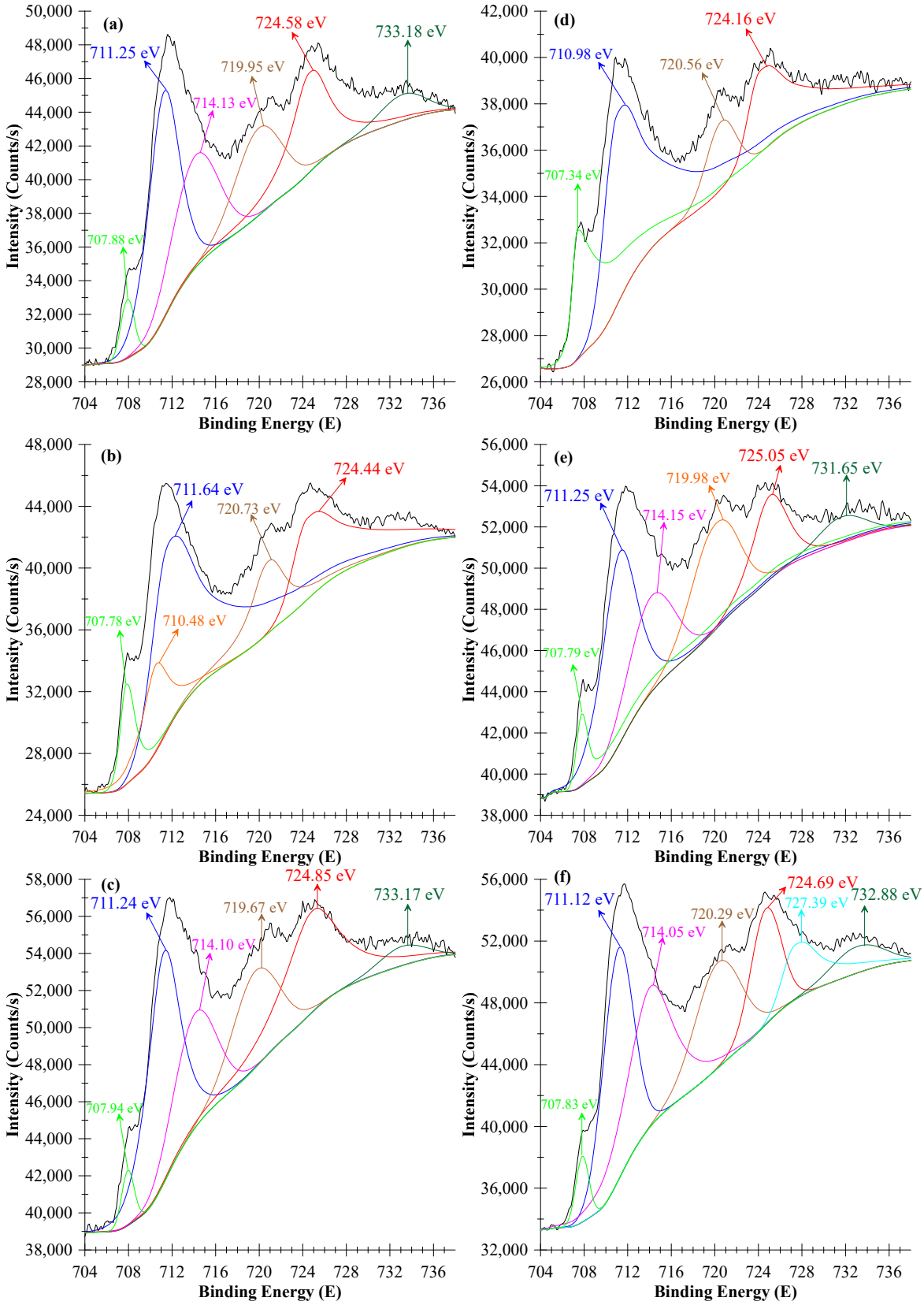



**Figure 12.** XPS spectrum of Fe 2p solid residues obtained at (**a**) 140 °C, (**b**) 160 °C, (**c**) 180 °C, (**d**) 0.8 MPa, (**e**) 1.0 MPa, and (**f**) 2.0 MPa at 700 rpm after 30 min of leaching.

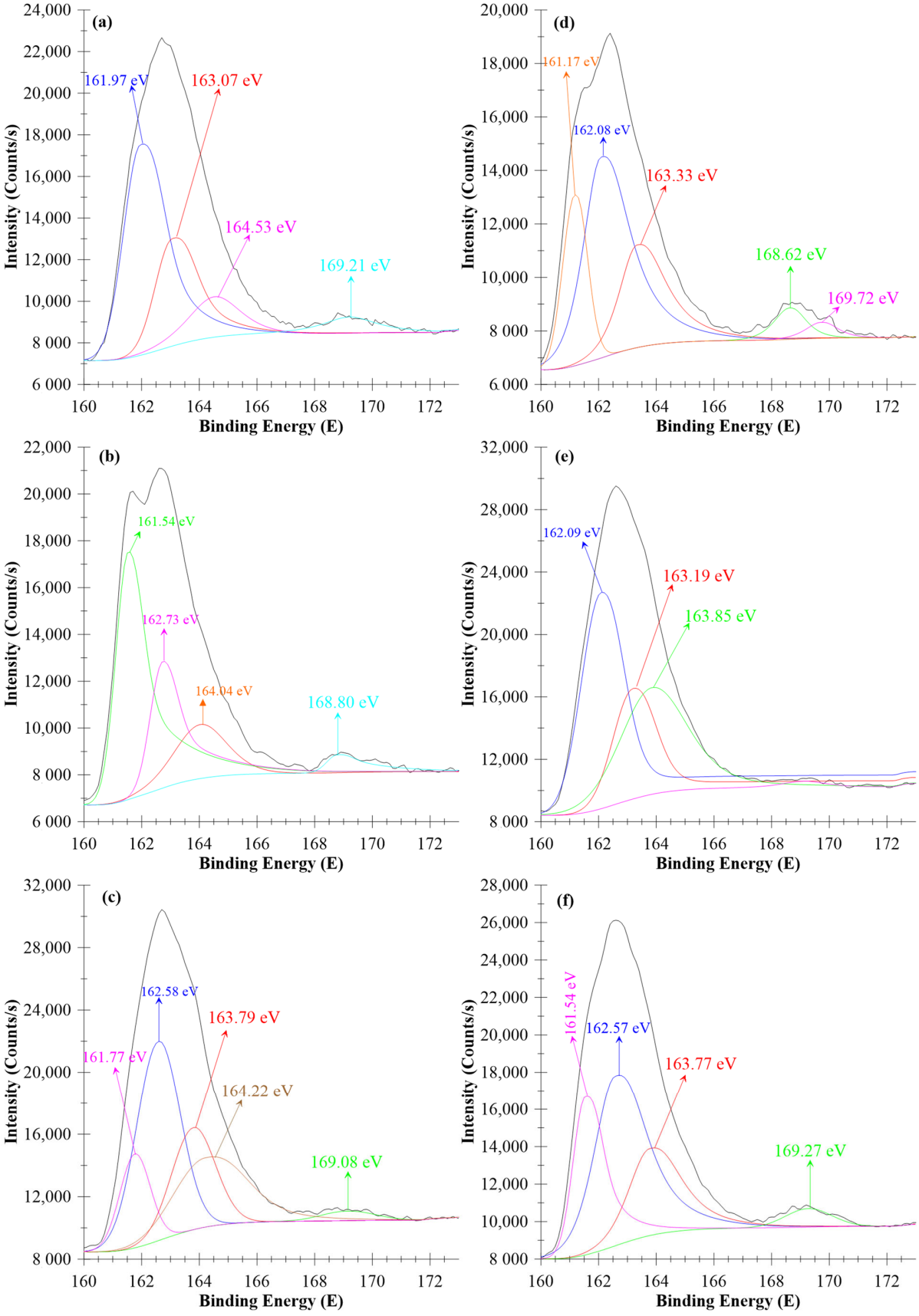



**Figure 13.** XPS spectrum of S 2p solid residues obtained at (**a**) 140 °C, (**b**) 160 °C, (**c**) 180 °C, (**d**) 0.8 MPa, (**e**) 1.0 MPa, and (**f**) 2.0 MPa at 700 rpm after 30 min of leaching.

On the other hand, a typical high-resolution spectrum of Fe 2p for un-leached chalcopyrite is presented in Figure 9a. The spectrum shows two strong peaks of Fe 2p3/2 and Fe 2p1/2 at 711.96 and 725.10 eV, respectively, and a peak at 707.62 eV was found. As Chen et al. and Khoshknoo et al. [6,25] mentioned, the peaks around 707.00 and 711.00 eV indicated the relevant compounds with the 2p3/2 binding energy of $Fe^{2+}$ and $Fe^{3+}$, respectively. These results were in agreement with the findings shown in the Cu 2p spectrum, which indicated that Fe existed as $Fe^{2+}$ and $Fe^{3+}$ in the chalcopyrite lattice [6]. Figure 10a illustrates the high-resolution spectrum of S 2p for the original chalcopyrite sample. The S 2p peaks occurred as doublets with S 2p3/2 and S 2p1/2 due to spin-orbit splitting [2,22]. It can be seen from Figure 10a that there were several relatively prominent peaks at 161.27, 162.33, 163.46, 169.08, and 170.35 eV in the un-leached chalcopyrite surface. It has been reported that the S 2p3/2 peak centered at the binding energy of 161.00–161.50 eV [2,3,22,25], 162.10–162.50 eV, and 163.00–163.90 eV corresponds to the values of monosulfide ($S^{2-}$), disulfide ($S_2{}^{2-}$), and polysulfide ($S_n{}^{2-}$), respectively. Moreover, the XPS spectrum fitted at the binding energy of 169.08 and 170.35 eV could be assigned to sulfate ($SO_4{}^{2-}$), indicating the chalcopyrite sample was slightly oxidized [6,26,27]. Hence, it was confirmed that monosulfide, disulfide, polysulfide, and sulfate were the main sulfur species on the un-leached chalcopyrite surface.

The high-resolution spectrum of Cu 2p for solid residues is given in Figure 11a–f. As can be seen from the results, similar Cu 2p spectrums were detected on the residues obtained after 30 min of leaching compared with that of the un-leached chalcopyrite surface, due to the leaching rate of copper being less than 50%, even under the most consequential conditions. Since the satellite peak was always present in the Cu 2p spectrum even after 30 min of leaching, it was difficult to confirm whether the copper species originated from the original chalcopyrite or the newly released compounds. However, the formation of CuS on the surface of oxidized chalcopyrite has been detected by other researchers [3,28,29]. As shown in Figure 8c,d, there were no significant binding energy peaks found on the surface of the residues obtained after 60 and 90 min of leaching, indicating that nearly all of the chalcopyrite was extracted in the solution, which was consistent with the leaching result of over 95%. Again, the CuL3M45M45 values were centered around 568.5 eV (Table 2), which could be assigned to CuS, but not $CuS_2$ [3,24].

Figure 12a–f shows the high-resolution spectrum of Fe 2p for the solid residues obtained after leaching at certain conditions. It can be seen from Figures 10a and 12a–f that there were no more differences between the Fe 2p spectrum in non-dissolved chalcopyrite and residues obtained after 30 min of leaching, while the copper leaching rate from chalcopyrite was lower than 50%, indicating that chalcopyrite was still the major phase of the residue and coexisted with other newly generated components, such as hematite. However, the peaks centered around 707.62 eV disappeared, and a new peak located at about 710.28 eV was found when the leaching time extended to 60 or 90 min. The peaks at 710.30 eV could be attributed to the Fe 2p3/2 peaks of $Fe_2O_3$, FeOOH or $Fe_3O_4$, which are all centered around 710.00 eV; therefore, it is not possible to distinguish between them. However, from the XRD analysis shown in Figure 3, the primary phase of the residue was $Fe_2O_3$, and no FeOOH or $Fe_3O_4$ was confirmed at all. Accordingly, the peaks at 710.30 eV could be attributed to the Fe 2p3/2 peaks of $Fe_2O_3$. Additionally, it must be pointed out that the Fe 2P3/2 peaks at 707.40 eV could be assigned to the binding energy of $Fe^{2+}$ species bonded to sulfur, e.g., FeS or $FeS_2$, which was 707.50 eV and 707.40 eV, respectively. Fortunately, the $FeS_2$ peaks were detected by the XRD analysis of the solid residues, which might be evidence that the Fe-S species was most likely $FeS_2$.

From the results of the S 2p spectra (see Figure 13a–f), it was shown that $S^0$ (164.00–164.50 eV) was detected in the residues obtained after 30 min leaching, which was in agreement with the reported value [26,30,31]. By contrast, the binding energy peaks during 160.00–166.00 eV disappeared with the extending leaching time to 60 or 90 min (see Figure 10c,d), and only the peaks centered at 168.85, 168.93, 170.07, and 170.21 eV (i.e., 168.00–170.00 eV) were found [2]. Additionally, the corresponding electronic peak

area around 169.00–190.00 eV in the S 2p high-resolution spectrum of the 30 min leaching residue was significantly increased [26]. Some studies have shown that the electronic peak corresponding to element S at 169.0 eV is $SO_4^{2-}$, which indicates that with the increase in leaching time, element S finally exists in the form of $SO_4^{2-}$ [32]. This phenomenon demonstrated that $S^0$, an intermediate product in the chalcopyrite leaching process, was generated and efficiently oxidized at relatively powerful conditions and changed to $SO_4^{2-}$. However, it must be pointed out that the $S^0$ is only an intermediate product, and it will be oxidized by the leaching even at a lower experimental condition set, meaning only a tiny amount of it will remain on the mineral surface, which is why $S^0$ was not detected in residues by XRD in Figure 3.

### *3.4. The Proposed Dissolution and Passivation Mechanisms of Chalcopyrite*

The proposed dissolution and passivation mechanisms of chalcopyrite under pressurized oxidative conditions in water are shown in Figure 14. It must be pointed out that there was no pyrite present in the feed chalcopyrite samples, which has been reported as a sulfuric acid source for chalcopyrite leaching [1,19,33]. However, it was confirmed that chalcopyrite dissolution could be "switched on" without adding an acid or any acid source via the reaction given in (2). Meanwhile, the Cu was released into the solution, and hematite and sulfuric acid were generated. The produced sulfuric acid promoted chalcopyrite leaching and dissolved more $Cu^{2+}$ in the PLS according to reactions (3)–(6), including ferric sulfate ($Fe_2(SO_4)_3$), ferrous sulfate ($FeSO_4$), and even $S^0$. It is well known that ferric sulfate can also assist the dissolution of un-leached chalcopyrite through reactions (7) and (8), and is regenerated via reaction (9) from ferrous sulfate. As the chemical leaching, XRD, and XPS results showed, finally, the majority of ferric sulfate was hydrolyzed as hematite (see reaction (10)), which exhibited a "multi-sphere" and "honeycomb" structure (Figures 4f,g, 6, 7 and 14), and only around 13% of Fe ions were in the solution. The chemistry of chalcopyrite oxidation at pressurized water leaching conditions is more complex since a significant fraction of the sulfide is oxidized to elemental sulfur (possibly via reactions (4)–(6) and (8)) in the early stage of the dissolution process, which was confirmed by the XPS study. However, as the leaching process of chalcopyrite continues, the elemental sulfur is converted entirely to sulfate or sulfuric acid and proceeds via the typical reactions (11) and (12). Interestingly, pyrite, which was not present in the original sample, was detected by the XRD and XPS studies, indicating that pyrite might have been formed as an intermediate product via reaction (12). The pyrite could be a source of $H_2SO_4$ and ferric sulfate via reaction (12), enhancing copper dissolution from chalcopyrite under pressurized water leaching conditions. Moreover, The XRD, SEM, and XPS data suggested that a large proportion of the chalcopyrite was converted to a covellite-like phase (via the proposed reactions (14)–(17)) during the pressurized water leaching period. This finding suggested that not all of the copper dissolved in the solution via $CuFeS_2 \rightarrow Cu^{2+}$, but that some of it proceeded via the mineral phase transformation of $CuFeS_2 \rightarrow CuS \rightarrow Cu^{2+}$. The conversion to covellite yields cupric ions and elemental sulfur via reactions (18) and (19). It must be pointed out that there were several passivation layers, such as hematite, pyrite, and covellite, generated during chalcopyrite pressurized water leaching; however, none of them covered the un-leached mineral surface or inhibited chalcopyrite dissolution, as long as the agitation speed and leaching time were maintained over 700 rpm and 60 min, respectively.

$$2CuFeS_2 + 8.5O_2 + 2H_2O \rightarrow 2CuSO_4 + Fe_2O_3 + 2H_2SO_4, \quad (2)$$

$$2CuFeS_2 + 8.5O_2 + H_2SO_4 \rightarrow 2CuSO_4 + Fe_2(SO_4)_3 + H_2O, \quad (3)$$

$$2CuFeS_2 + 2.5O_2 + 2H_2SO_4 \rightarrow 2CuSO_4 + Fe_2O_3 + 4S0 + 2H_2O, \quad (4)$$

$$CuFeS_2 + 2.5O_2 + H_2SO_4 \rightarrow CuSO_4 + FeSO_4 + H_2O + S^0, \quad (5)$$

$$2CuFeS_2 + 2.5O_2 + 5H_2SO_4 \rightarrow 2CuSO_4 + Fe_2(SO_4)_3 + 4S0 + 5H_2O, \quad (6)$$

$$2CuFeS_2 + 16Fe2(SO_4)_3 + 16H_2O \rightarrow 2CuSO_4 + 34FeSO_4 + 16H_2SO_4, \quad (7)$$

$$CuFeS_2 + 2Fe_2(SO_4)_3 \rightarrow CuSO_4 + 5FeSO_4 + 2S^0, \quad (8)$$

$$2FeSO_4 + 0.5O_2 + H_2SO_4 \rightarrow Fe_2(SO_4)_3 + H_2O, \quad (9)$$

$$Fe_2(SO_4)_3 + 3H_2O \rightarrow Fe_2O_3 + 3H_2SO_4, \quad (10)$$

$$2S^0 + 3O_2 + 2H_2O \rightarrow 2H_2SO_4, \quad (11)$$

$$2S^0 + 3FeSO_4 \rightarrow FeS_2 + Fe_2(SO_4)_3, \quad (12)$$

$$2FeS_2 + 7.5O_2 + H_2O \rightarrow Fe_2(SO_4)_3 + H_2SO_4, \quad (13)$$

$$CuFeS_2 + 0.5O_2 + H_2SO_4 \rightarrow CuS + FeSO_4 + S0 + H_2O, \quad (14)$$

$$CuFeS_2 + CuSO_4 \rightarrow 2CuS + FeSO_4, \quad (15)$$

$$CuFeS_2 + Fe_2(SO_4)_3 \rightarrow CuS + 3FeSO_4 + S^0, \quad (16)$$

$$S^0 + CuSO_4 + 2FeSO_4 \rightarrow CuS + Fe_2(SO_4)_3, \quad (17)$$

$$CuS + 2Fe_2(SO_4)_3 \rightarrow CuSO_4 + 4FeSO_4 + 2S^0, \quad (18)$$

$$CuS + 0.5O_2 + H_2SO_4 \rightarrow CuSO_4 + S0 + H_2O. \quad (19)$$

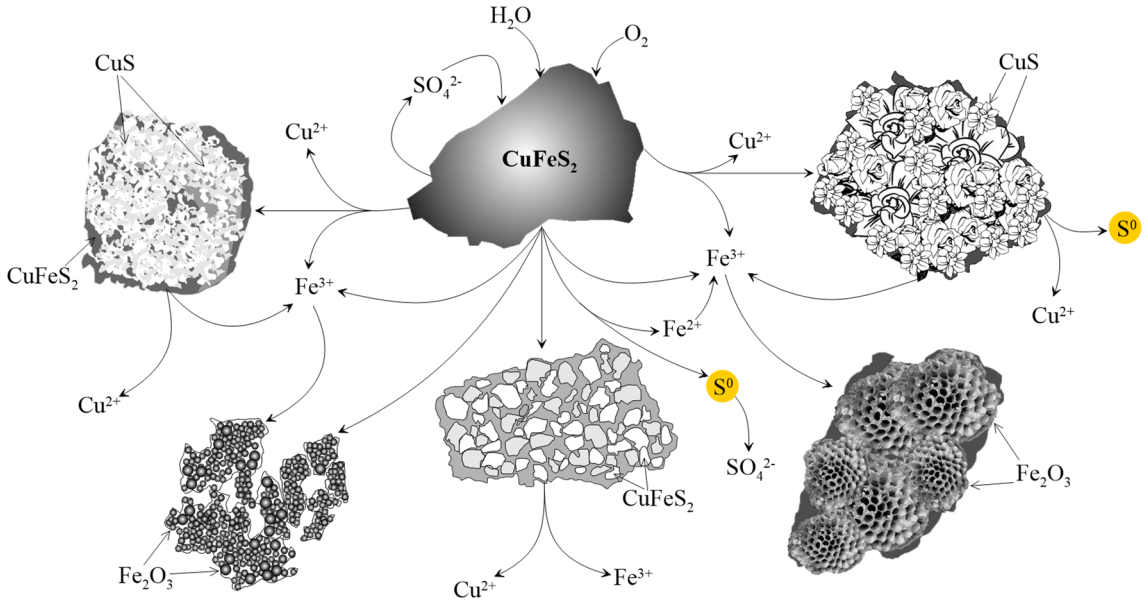



**Figure 14.** The proposed dissolution and passivation mechanisms of chalcopyrite leaching in an $O_2$–$H_2O$ system.

## 4. Conclusions

This work conducted chemical leaching, X-ray diffraction, and X-ray photoelectron spectroscopy studies to understand chalcopyrite's dissolution and passivation mechanisms under pressurized oxidative conditions in water. The results can be summarized as follows.

(1) The chemical leaching study showed that it was possible to dissolve copper from chalcopyrite in an $O_2$–$H_2O$ system, with the copper leaching rate reaching 96.4% under the optimal conditions of a temperature of 180 °C, a total pressure of 1.5 MPa, a stirring speed of 900 rpm, and a leaching time of 90 min.

(2) The XRD, SEM, and XPS data suggested that a large proportion of the chalcopyrite was dissolved in the solution via the mineral phase transformation of $CuFeS_2 \rightarrow Cu^{2+}$ and $CuFeS_2 \rightarrow CuS \rightarrow Cu^{2+}$, i.e., some of the chalcopyrite directly leached into the solution as $Cu^{2+}$ and some of it was first converted to CuS and then to $Cu^{2+}$.
(3) The primary passivation layers during chalcopyrite pressurized water leaching were hematite, pyrite, and covellite; however, none of them covered the un-leached mineral surface or inhibited chalcopyrite dissolution, as long as the agitation speed and leaching time were maintained over 700 rpm and 60 min, respectively.

**Author Contributions:** B.H. conceived and designed the experimental methodology; L.J. and H.L. performed the experiments and analyzed the data. B.H. contributed reagents and materials. All authors have read and agreed to the published version of the manuscript.

**Funding:** This research was funded by the Outstanding Young Talents Project of the University of Science and Technology Liaoning grant number 2021YQ05.

**Data Availability Statement:** The data that support the findings of this study are available from the corresponding author, upon reasonable request.

**Acknowledgments:** This work was supported by the Outstanding Young Talents Project of the University of Science and Technology Liaoning (No. 2021YQ05).

**Conflicts of Interest:** The authors declare no conflict of interest.

## References

1. Han, B.S.; Altansukh, B.; Haga, K.; Stevanovic, Z.; Jonovic, R.; Avramovic, L.; Urosevic, D.; Takasaki, Y.; Masuda, N.; Ishiyama, D.; et al. Development of copper recovery process from flotation tailings by a combined method of high-pressure leaching solvent extraction. *J. Hazard. Mater.* **2018**, *352*, 192–203. [CrossRef]
2. Tehrani, M.E.H.N.; Naderi, H.; Rashchi, F. Electrochemical study and XPS analysis of chalcopyrite dissolution in sulfuric acid in the presence of ethylene glycol. *Electrochim. Acta* **2021**, *369*, 137663. [CrossRef]
3. Ghahremaninezhad, A.; Dixon, D.G.; Asselin, E. Electrochemical and XPS analysis of chalcopyrite (CuFeS2) dissolution in sulfuric acid solution. *Electrochim. Acta* **2013**, *87*, 97–112. [CrossRef]
4. Ghomi, M.A.; Mozammel, M.; Moghanni, H.; Shahkar, L. Atmospheric leaching of chalcopyrite in the presence of some polar organic reagents: A comparative study and optimization. *Hydrometallurgy* **2019**, *189*, 105120. [CrossRef]
5. Sahlabad, M.K.; Javanshir, S.; Honarmand, M. Improvement in atmospheric leaching of chalcopyrite concentrate using a new environmentally-friendly ionic liquid. *Hydrometallurgy* **2022**, *211*, 105893. [CrossRef]
6. Chen, G.B.; Sun, J.R.; Yang, H.Y.; Ma, P.C.; Gao, S.X. Rapid Atmospheric Leaching of Chalcopyrite Using a Novel Reagent of Trichloroisocyanuric Acid. *Minerals* **2021**, *11*, 1012. [CrossRef]
7. Bai, Y.L.; Wang, W.; Xie, F.; Lu, D.K.; Jiang, K.X.; Dreisinger, D. In-situ electrochemical study of chalcopyrite pressure oxidation leaching from 110 degrees C to 150 degrees C under saturated vapor pressure. *Arab. J. Chem.* **2022**, *15*, 104139. [CrossRef]
8. Ji, G.X.; Liao, Y.L.; Wu, Y.; Xi, J.J.; Liu, Q.F. A Review on the Research of Hydrometallurgical Leaching of Low-Grade Complex Chalcopyrite. *J. Sustain. Metall.* **2022**, *8*, 964–977. [CrossRef]
9. Mojtahedi, B.; Rasouli, S.; Yoozbashizadeh, H. Pressure Leaching of Chalcopyrite Concentrate with Oxygen and Kinetic Study on the Process in Sulfuric Acid Solution. *Trans. Indian Inst. Met.* **2020**, *73*, 975–987. [CrossRef]
10. Turan, M.D.; Sari, Z.A.; Nizamoglu, H. Pressure leaching of chalcopyrite with oxalic acid and hydrogen peroxide. *J. Taiwan Inst. Chem. Eng.* **2021**, *118*, 112–120. [CrossRef]
11. Abdelraheem, M.T.O.; Agacayak, T. Investigation of the Effect of Some Polar Organic Solvents on the Leaching and Dissolution Kinetics of Chalcopyrite in Hydrogen Peroxide and Sulfuric Acid Solution. *Bull. Chem. Soc. Ethiop.* **2023**, *37*, 779–788. [CrossRef]
12. Ruiz-Sanchez, A.; Lazaro, I.; Lapidus, G.T. Improvement effect of organic ligands on chalcopyrite leaching in the aqueous medium of sulfuric acid-hydrogen peroxide-ethylene glycol. *Hydrometallurgy* **2020**, *193*, 105293. [CrossRef]
13. Hernandez, P.; Gahona, G.; Martinez, M.; Toro, N.; Castillo, J. Caliche and Seawater, Sources of Nitrate and Chloride Ions to Chalcopyrite Leaching in Acid Media. *Metals* **2020**, *10*, 551. [CrossRef]
14. Moraga, G.A.; Jamett, N.E.; Hernandez, P.C.; Graber, T.A.; Taboada, M.E. Chalcopyrite Leaching with Hydrogen Peroxide and Iodine Species in Acidic Chloride Media at Room Temperature: Technical and Economic Evaluation. *Metals* **2021**, *11*, 1567. [CrossRef]
15. Castellon, C.I.; Hernandez, P.C.; Velasquez-Yevenes, L.; Taboada, M.E. An Alternative Process for Leaching Chalcopyrite Concentrate in Nitrate-Acid-Seawater Media with Oxidant Recovery. *Metals* **2020**, *10*, 518. [CrossRef]
16. Hernandez, P.C.; Taboada, M.E.; Herreros, O.O.; Graber, T.A.; Ghorbani, Y. Leaching of Chalcopyrite in Acidified Nitrate Using Seawater-Based Media. *Minerals* **2018**, *8*, 238. [CrossRef]

17. Chindo, S.Y.; Omoniyi, K.I.; Agbaji, E.B.; Dallatu, Y.A.; Baba, A.A. Leaching of Copper from a Nigerian Chalcopyrite-Rich Siderite Ore by Ammonia-Ammonium Sulphate Solutions. *Min. Met. Explor.* **2023**, *40*, 161–169. [CrossRef]
18. Toro, N.; Pérez, K.; Saldaña, M.; Jeldres, R.I.; Jeldres, M.; Cánovas, M. Dissolution of pure chalcopyrite with manganese nodules and waste water. *J. Mater. Res. Technol.* **2020**, *9*, 798–805. [CrossRef]
19. Ji, G.X.; Liao, Y.L.; Xi, J.J.; Liu, Q.F.; Wu, Y.; Ma, H.F.; Li, J.L. Behavior and Kinetics of Copper During Oxygen Pressure Leaching of Complex Chalcopyrite Without Acid. *J. Sustain. Metall.* **2023**, *9*, 350–362. [CrossRef]
20. McDonald, R.; Muir, D. Pressure oxidation leaching of chalcopyrite. Part I. Comparison of high and low temperature reaction kinetics and products. *Hydrometallurgy* **2007**, *86*, 191–205. [CrossRef]
21. Chen, Y.; Chen, X.M.; Peng, Y.J. The depression of molybdenite flotation by sodium metabisulphite in fresh water and seawater. *Miner. Eng.* **2021**, *168*, 106939. [CrossRef]
22. Wang, J.; Gan, X.W.; Zhao, H.B.; Hu, M.H.; Li, K.Y.; Qin, W.Q.; Qiu, G.Z. Dissolution and passivation mechanisms of chalcopyrite during bioleaching: DFT calculation, XPS and electrochemistry analysis. *Miner. Eng.* **2016**, *98*, 264–278. [CrossRef]
23. Delgado, J.; de Delgado, G.; Quintero, M.; Woolley, J. The crystal structure of copper iron selenide, $CuFeSe_2$. *Mater. Res. Bull.* **1992**, *27*, 367–373. [CrossRef]
24. Ghahremaninezhad, A.; Asselin, E.; Dixon, D.G. Electrodeposition and Growth Mechanism of Copper Sulfide Nanowires. *J. Phys. Chem. C* **2011**, *115*, 9320–9334. [CrossRef]
25. Khoshkhoo, M.; Dopson, M.; Shchukarev, A.; Sandström, Å. Chalcopyrite leaching and bioleaching: An X-ray photoelectron spectroscopic (XPS) investigation on the nature of hindered dissolution. *Hydrometallurgy* **2014**, *149*, 220–227. [CrossRef]
26. Chanturia, V.A.; Bunin, I.Z.; Ryazantseva, M.V.; Khabarova, I.A. X-Ray photoelectron spectroscopy-based analysis of change in the composition and chemical state of atoms on chalcopyrite and sphalerite surface before and after the nanosecond electromagnetic pulse treatment. *J. Min. Sci.* **2013**, *49*, 489–498. [CrossRef]
27. Sandström, Å.; Shchukarev, A.; Paul, J. XPS characterisation of chalcopyrite chemically and bio-leached at high and low redox potential. *Miner. Eng.* **2005**, *18*, 505–515. [CrossRef]
28. Córdoba, E.; Muñoz, J.; Blázquez, M.; González, F.; Ballester, A. Leaching of chalcopyrite with ferric ion. Part II: Effect of redox potential. *Hydrometallurgy* **2008**, *93*, 88–96. [CrossRef]
29. Majuste, D.; Ciminelli, V.S.T.; Osseo-Asare, K.; Dantas, M.S.S.; Magalhaes-Paniago, R. Electrochemical dissolution of chalcopyrite: Detection of bornite by synchrotron small angle X-ray diffraction and its correlation with the hindered dissolution process. *Hydrometallurgy* **2012**, *111*, 114–123. [CrossRef]
30. Harmer, S.L.; Thomas, J.E.; Fornasiero, D.; Gerson, A.R. The evolution of surface layers formed during chalcopyrite leaching. *Geochim. Cosmochim. Acta* **2006**, *70*, 4392–4402. [CrossRef]
31. Muir, H.W.N.I.J. Oxidation states and speciation of secondary products on pyrite and arsenopyrite reacted with mine waste waters and air. *Mineral. Petrol.* **1998**, *62*, 123–144.
32. Bai, Y.L.; Wang, W.; Xie, F.; Lu, D.K.; Jiang, K.X. Effect of temperature, oxygen partial pressure and calcium lignosulphonate on chalcopyrite dissolution in sulfuric acid solution. *Trans. Nonferrous Met. Soc. China* **2022**, *32*, 1650–1663. [CrossRef]
33. Han, B.; Altansukh, B.; Haga, K.; Takasaki, Y.; Shibayama, A. Leaching and Kinetic Study on Pressure Oxidation of Chalcopyrite in H2SO4 Solution and the Effect of Pyrite on Chalcopyrite Leaching. *J. Sustain. Metall.* **2017**, *3*, 528–542. [CrossRef]


**Disclaimer/Publisher's Note:** The statements, opinions and data contained in all publications are solely those of the individual author(s) and contributor(s) and not of MDPI and/or the editor(s). MDPI and/or the editor(s) disclaim responsibility for any injury to people or property resulting from any ideas, methods, instructions or products referred to in the content.